



11may2018

Dear Editor: With respect to:

Title: Turbulent Length Scales in a Fast-flowing, Weakly Stratified, Strait: Cook Strait, New Zealand

Author(s): Craig L. Stevens

MS No.: os-2017-30

Please Find the Following:

- Response to Reviewer 1
- Response to Reviewer 2
- Tracked Changes Version of Manuscript

I believe this work documents rarely recorded measurements from a novel location, yielding new insight into aspects of mixing in the ocean with general applicability beyond the sample location. I thank you and the Reviewers for the time taken to improve the manuscript.

Best regards

A handwritten signature in black ink, appearing to read "Craig Stevens".

Craig Stevens

## Response to Reviewer 1 comments on Stevens (2017) Turbulent length scales in a fast-flowing, weakly-stratified Strait: Cook Strait, New Zealand. (original reviewer comments in black).

This is an interesting paper reporting measurements of turbulence in a very energetic flow through ocean straits, in this case Cook Strait N.Z. Such measurements are relatively rare and this therefore represents an interesting addition to the literature on direct measurements of ocean turbulence in energetic flow. That said, the paper is poorly presented with some important details about the measurements not included in the paper, and even some typographical errors. These issues need to be addressed before the paper is suitable for publication.

*I thank the Reviewer for their very helpful and clearly knowledgeable comments and suggestions. The recent emergence of multiple papers in the literature on aspects of this topic is further evidence that this research theme is important and widely applicable. The following responds to their points. The lack of inclusion of measurement details is responded to below and describes the associated modifications to the revised manuscript. With regard to the point about poor presentation, a number of typos have been cleaned up. As well as this, their comments have motivated a substantial number of improvements.*

### Detailed comments:

- P1,L24 Waterhouse et al 2014 - *thanks, corrected.*
- P1,l27 Wesson and Gregg (1994) report measurements in Straits of Gibralter, so why is this "... (a) coastal environment". Koch-Larrouy et al (2015) (DSR, 106:136-153) is also relevant here. – *fair enough, I think the point of difference relates to what is a coastal environment and the mechanics of "influence". The initial reference was to bring attention to the effect of strong tidal mixing but I am happy with the reviewer's suggestion as well and additional reference that connects to high trophic levels (Scott et al. 2010) and have modified the text accordingly.*
- P2, L20 . Energy bearing scale. Why is  $LT$  contained by  $LO$  , they are independent lengthscales? *This is of course a key question to ask and is at the heart of the study and many others. The Reviewer asks in what sense are they independent?  $LT$  is empirical and  $Lo_z$  is a scaling argument - but of the same mechanics. What about "constrained by the  $Lo_z$ "? The relationship between  $LT$  and  $Lo_z$  is key to the manuscript and many papers that seek to quantify dissipation rate from overturn scale. I have changed to "constrained" and return to this dependence in the Discussion – "The calculated  $Lo_z$ , on the other hand, is not actually physically constrained and in several instances it exceeds the water depth".*
- P5, L18- "The microstructure data were processed in the usual ways resolving the dissipation" is insufficient. Is the author speaking of using the Naysmith empirical spectrum? More detail is needed here. Bluteau et al (2017, JTECH, 34: 2283-2293) provides an extensive review of processing methods for free-fall profilers, and also provides insight into how to process fast-response temperature measurements, and it may well be possible to apply these ideas here. See below. *Reviewer Two highlights this also. This is a debatable point as the field has evolved that there is now a consistent set of hardware and data processing available. For example, the canonical Wesson and Gregg 1994 paper addresses such*

points of clarity and so the numerous studies in the intervening quarter of a century fill in many of these issues. For example, Bluteau et al. 2017 refers to an earlier paper for shear microstructure methods. On reflection, I should not have used the phrase "in the usual way". The Reviewer is correct in that there are always points of clarity and interest in following through on these aspects. In acceding to the Reviewer's point, I now include the reference to Bluteau et al. (2017) which was published after the initial submission of the present manuscript and include additional information regarding the processing. I do note that the original manuscript included a figure and discussion of variability in drop speed which is rarely discussed in available studies. I have made this contribution clearer in the revision.

- P5, l23 what is xxx? *Thanks for spotting this as there were some version control issues. This returns to the point above about the relationship between LT and LO. The amended text now says "One might expect overturns, as identified using the LT, to be equal to, or smaller than LOz. Dillon (1982) observed the ratio to be LT/LOz =0.8. This calculation struggles with regions of weak stratification where locally-small N2 drives a very large scale. This makes sense as weak stratification fails to retard turbulence. However, it can lead to non-physical outcomes as the scale will eventually exceed water depth."*
- P6, L4 Ranges of  $\Gamma$  are missing. See Bluteau et al (2017) and references therein. *Thanks. The ranges weren't missing, they were not specified. This is helpful as the Bluteau reference was not available at the time of writing the initial manuscript. Although to be fair this reference doesn't clearly identify the ranges specifically – it's concluding remarks say "The estimated Rif varied over almost two orders of magnitude with a median Rif not significantly different from the canonical value of 0.17. The median Rif obtained from either technique did not differ significantly from this value, although the median Rif obtained from the fitted chi estimates were slightly larger the median Rif obtained from the integrated chi estimates". The text has now been amended in a number of places to highlight the results of Bluteau et al (2017).*
- P7, L5 The fact that the Strait is not well mixed suggests that the vertical diffusion time scale  $H2 Kz$  is long compared to advection times in the Strait? Assuming here that advection is re-establishing the vertical gradient? This is discussed later in paper, but argument is confusing. *The point is important because, in an applied sense, this is a key aspect of the location and experiment. A number of references assume because it is fast flowing and clearly turbulent that it homogenizes the water column. This is not supported by the observations. These observations come from the strait narrows and so presumably represent the most energetic conditions. The Reviewer suggests that it is restratification due to advection. This is possible, but given the spatial heterogeneity and relatively fast transit time it is also possible that the water column simply doesn't have time to homogenize as suggested by the scaling in the discussion. This point is now clarified in both the Results and Discussion which has been amended to say "This suggests that, at these most energetic of mixing conditions, we should not expect to see a stratified water column as it should get mixed over the multiple tidal cycles it takes for water to clear the strait. The bulk top-bottom observations Fig 5) counter this as, for some of the year at least, there is clearly a scalar gradient. Possibly, the observations need to be restructured and collected drifting with the flow to better follow the evolution of mixing."*

- P7, l20. The usual argument is the dissipation rate is dependent on the intensity of the background shear  $S$ . Why is it dependent on  $N$ ? *The  $N$  is used here to delineate layers in the water column (at least on a profile-by-profile basis). The text originally was designed to indicate that the dissipation rate and stratification structure were consistent. I agree with the Reviewer that this terminology could be misleading and have reworked the text to not imply direct causality.*
- P7, l23 One has to wonder how meaningful is the calculation of the Thorpe scale  $LT$  in this situation. It is a strongly advective situation and vertical stratification is (relatively) weak, so how do these effects conspire here? Some estimates of accuracy of  $LT$  scale calculations would be useful, particularly as here we find the scales are large compared to the total depth? *This is an excellent point and one that has been explored in the wider analysis of the problem but not included in the initial manuscript. I believe the Reviewer is getting at the issue that such a large overturn will have time to be affected by the background flow. It is not clear to me that it affects the "accuracy" of the  $LT$  but rather it affects what the  $LT$  actually means. This is now considered in the Discussion which says ..."While the  $LT$  never approaches the full water depth, they are large given the flow speeds. Stevens (2014) measured velocity shear at bulk scales (i.e. resolved from 8 m ADCP bins) reaching as high as 0.01 s<sup>-1</sup>. The velocity variation over an eddy of  $LT$ =100 m in a flow with a velocity shear of 0.01 s<sup>-1</sup> is 1 m s<sup>-1</sup>. This is comparable, but not greater than, background speeds suggesting that it might influence the degree of isotropy by straining eddy structure in the horizontal direction."*
- P8, l2 But how is  $KZ$  computed here? Large values of  $KZ = 10^{-1} \text{ m}^2 \text{s}^{-1}$  have been reported by Bluteau et al (2017), but they argue these high values are much more reliably estimated from the temperature spectra than the velocity spectra. As Bluteau et al (2016, JTECH, 33:713-722) argue integration methods are only robust if  $\epsilon \leq 10^{-6} \text{ m}^2 \text{s}^{-1}$ . Author should consider this point carefully. I assume in all the processing that the author has used  $\Gamma = 0.2$ ? While on average this may be globally true, the flow in Cook Strait seems very unusual with very high mean velocities and very high values of  $Reb$  in Figure 11, for example. The point being that consistently here possibly  $\Gamma \neq 0.2$  and it may be very misleading to assume that in the present observations – see Bluteau et al Fig 4.? So in Figures 7,8 and 9 is  $KZ$  to be believed? There seems only one way to check this: independently compute  $KZ$  from the temperature field, without any a priori assumption on the value of  $\Gamma$ .  
*The Reviewer rightly picks up on one of the major themes in ocean turbulence – the efficiency of mixing – this is too big for this manuscript and dataset which focuses on the  $LOz/LT$  question. The Reviewer also picks up on the unusual nature of the flow with its high mean velocities. The changes I have made in response are to remove panel (b) of previous Fig. 10. (the  $Kz$  distribution) and replace the axes in Fig 7, 8 & 9 with  $0.2\epsilon/N^2$  and then expanded the Discussion. Given the bounds suggested by Bluteau et al 2017 there should still be meaning given the dynamic range observed. This enables the later discussion to be augmented as well as emphasised what future work is required. The revised text now all considers the related point made by Smyth et al. 2001, based on DNS of patches, which demonstrates the order of magnitude variability in  $LO/LT$  over the lifetime of the turbulent event.*
- P9, l17 The range of  $Reb$  estimates is 2 orders of magnitude? Figure 11 suggests more than 4 orders of magnitude?

*Agreed, the original text was misleading and has now been clarified. It now states... "In the present Cook Strait data, the majority of Reb estimates exceed 100, with the peak of the distribution being around  $5 \times 10^4$  two orders of magnitude with the peak of the distribution around  $5 \times 10^4$ . (Figure 11). However, maximal values exceed  $10^7$ , which is primarily due to the small N."*

- Fig 12 suggests a very poor correlation between  $Lo$  and  $Lt$  – its log-log after all! *I accept the Reviewer's point that the best-fit distribution is centred on some widely spread data points. As noted by the Reviewer these variables are "independent" in the sense that they are derived from different components of the profile data. However, this level of variability is consistent with the spread of results of Wesson and Gregg (1994) all the more so because we calculate  $LT$  using the microstructure sensors allowing for a much smaller minimum lengthscale. Given that these data are at one limit of ocean energetics I believe we have to be careful about rejecting data because they don't conform to expectations. I have added material to the first subsection of the discussion on this point.*
- P11, l13 Maybe it simply means that the gamma is not 0.2, irrespective of the  $Re$ ? *Is the Reviewer suggesting that the  $Kz$  is different enough to make the scaling argument not useful? Given that the scaling is linear in  $\Gamma$  and the present homogenization time is 25 hours, this suggests that the  $Kz$  might be out by a factor of 5 say - i.e. homogenization takes 5 hours. The text is now amended to connect this point with that raised above around  $\Gamma=0.2$ . It says "The  $\Gamma=0.2$  "constant" is a clear point of contention in the literature (e.g. Bluteau et al. 2013; Mashayek et al. 2013). Bluteau et al. (2017) develops an approach that takes microstructure profiles and resolves the diffusivity "directly" fitting a model for dissipation of thermal variance to the convective-inertial subrange (i.e. lower wavenumbers than the dissipation scale). The Bluteau et al. (2017) analysis suggests that improved estimation of the thermal diffusivity indicates that the fixed mixing coefficient might underestimate mixing by a factor of 5 in the mean especially for the more turbulent events. Extending this by applying the Osborne diffusivity method sees an average diffusivity is around  $0.04 \text{ m}^2 \text{ s}^{-1}$  and exceeding  $1 \text{ m}^2 \text{ s}^{-1}$  (Figure 10b). One might expect a 300 m water column to then be homogenised in a time  $(L^2/Kz)^{1/2} = 25$  hours, but this might be as little as 5 hours if the Bluteau et al. (2017) increased estimate of  $Kz$  were to hold."*
- P14 line 10 where is the Hogg reference cited.? *Thanks for spotting this missing reference. This has now been included (Table 1 caption and Discussion).*

## References

Scott, B.E., Sharples, J., Ross, O.N., Wang, J., Pierce, G.J. and Camphuysen, C.J., 2010. Sub-surface hotspots in shallow seas: fine-scale limited locations of top predator foraging habitat indicated by tidal mixing and sub-surface chlorophyll. *Marine Ecology Progress Series*, 408, pp.207-226.

**Response to Reviewer 2 comments on Stevens (2017) Turbulent length scales in a fast-flowing, weakly-stratified Strait: Cook Strait, New Zealand. (original reviewer comments in black).**

- The manuscript discuss direct measurements of turbulent quantities in Cook Strait. Considering that such data are relatively scarce in oceanography and can be interpreted in a broader context, the reported data are valuable.

*I am pleased the Reviewer sees the value of the data being in a wider context and not site-specific. Their comments have motivated a substantial number of improvements.*

- The central issue of this manuscripts and its main message is about the comparison between the Thorpe and Ozmidov scales. Unfortunately, the discussion itself is rather short and poorly documented (three references). More efforts should be put in the analysis around figures 12, 13 and 14. The manuscript will be greatly improved by a better focus on this scientific issue. In particular, can the data shed new light on the claim (Mater, 2013) that  $LT \sim LO$  with  $N.k \sim \epsilon$ ?

*I have now expanded the Discussion. The limited number of references discussed originally was partly related to the limited directly related studies. In addition, one of the key references in the Discussion is a synthesis (Mater et al 2015) so there is implicit connection to a wider literature. The discussion now includes material on the relative magnitudes of the LT and LO scales. It is difficult to make a direct dynamical comparison as the two studies do no overlap in scale – as is to be expected with the DNS approach. Certainly, the field observations do not exhibit the roll-off at larger LO. To be fair these authors, in the later 2015 paper, do move their perspective to ocean scales and this is where the present manuscript picks up the comparison. One of the additions made in response to the Reviewer's point, also from DNS – this time Smyth et al. 2001, demonstrates the order of magnitude variability in LO/LT over the lifetime of the turbulent event, something that the Mater et al 2013 paper doesn't clearly respond to.*

- The measurements themselves are presented with (too) many figures, but basic information is missing. Little is said, for instance, on the timing of the collected 34 profiles covering a very large period of time of 5 years. Processing of the microstructure data must be described or documented in a much more precise way than with sentences like "in the usual way" or "An approach".

*As noted in Response to Reviewer #1, additional details on sampling and microstructure analysis are now included. The profiles come from only a short window of 12 days within this longer period. Also, the driver is strongly tidal so periods between measurements should be irrelevant especially as the separation is between scene-setting broad scale information in the earlier data collection (where previous work demonstrated consistency from year to year) and the later microstructure work.*

*Details on the profiling timing is contained in Figure 6. This was erroneously not specifically referenced but was talked about in the previous version. I thank the Reviewer for spotting this and have now augmented the Methods section. The figure has been moved forward to Fig 2 and the associated text now says "The timing of the profiles during the 2012 sampling is shown in Figure 2. Long periods of contiguous sampling is difficult because a vessel suitably manoeuvrable to conduct the experiments is prone to weather limitations. Sampling over three days in 2012 centered on periods spanning northward, turning and southward tidal flows (Figure 2)."*

*In addition, The number of figures has been reduced by one – removing the Kz distribution and combining the eps and Re\_b figures.*

- Considering the fast flows in this region and the irregular topography, three-dimensional effects (e.g. horizontal advection) are anticipated and should be discussed.  
*The Reviewer makes a good point. This partly overlaps with a comment by Reviewer 1 about the veracity of the LT in such fast flowing waters. The text has now been amended to include discussion on this at the end of the first subsection in the Discussion. I argue, however, that the topography is not irregular at least in the region where data were collected. It is actually, over the distance travelled in any one tidal cycle, reasonably “regular” in the sense that there are no major changes in channel orientation and no submarine ridges running transverse to the flow (Fig. 1c). Evidence of this (i.e. lack of cross-strait eddies) is contained in the Strait being considered something of a bioregional barrier limiting across-strait connectivity (Forrest et al 2009). This is now included in the Discussion which says “the Strait has been identified as a dividing line in terms of ecological structure (e.g. Forrest et al 2009). The implication is that there is not a great deal of across strait transport. This supports the focus of the present work on the vertical structure. Furthermore, over the time it takes to drift through the strait all vessel tracks tended to be on an axis aligned with the strait. Over these scales of time and space the strait itself is bathymetrically reasonable consistent. It remains to conduct a study that will adequately quantify across-strait mixing and the associated drivers.”*
- Some of the (many) typos and formal problems to be fixed.
  - Page 3, line 4 : “velocity Sh” ! velocity shear ? *fixed*
  - Page 3, line 8 : “Do we actually observe high dissipation rates?” *fixed*
  - Bottom of page 5 and first paragraph of page 6 : please fill the gaps “xxx” and “X” “Y”. *fixed*
  - Please carefully check references : some of them are missing or unused (Gregg and Oszoy, 2002; Matter et al, 2003 or 2005; . . . ) *both now included*.
  - Figure 6 seems not to be cited / discussed in the text. *Thanks for spotting this – this has now been moved to Figure 2 and discussed at some length.*
  - Many figures are provided but with very little discussion. The ratio number of figures to Length of discussion seems to be rather low. *The revised Discussion is expanded to provide a more lengthy treatment of the data and the issues. In addition, the manuscript has been reduced by one figure.*
- In conclusion, the data are interesting but the manuscript should be better focused to avoid wild discussions of many details (e.g. on individual profiles taken at different (unknown) location and times) and come to solid conclusions.

*I thank the Reviewer for their suggestions and critique. The modified Discussion now focuses more specifically on the questions posed in the introduction and provides additional insight into the mechanical context and how this relates to the observed data shown in the figures. I do defend though the descriptions of the individual profiles which are there to serve as a context to talk about some of the actualities that can get lost when considering a scatter diagram covering many orders of magnitude and many hundreds of realisations. This helps the reader keep in mind that oceanic turbulence structure cannot be considered to be a series of disconnected experiments (as implied in Mater et al. 2013) but connected parts of a continuum. As noted above, to be fair these authors, in the later 2015 paper, do move their perspective to ocean scales and again this is where the present manuscript picks up the comparison. In regard*

*to the examination of selected individual profiles I took inspiration from the canonical Wesson & Gregg paper that included a small number of individual profiles to ground the later synthesis within the context of the source data. I note also that Mater et al 2015 look at selected patches. I certainly wouldn't argue that the entire manuscript be filled with such examination, but I believe it helps put the synthesis into better context. In addition, thanks in part to the points raised by the Reviewer, I believe the manuscript now comes closer to contributing to the "solid conclusions" they seek for questions at the forefront of ocean turbulence for some time now.*

#### References

- Forrest, B.M., Gardner, J. and Taylor, M.D., 2009. Internal borders for managing invasive marine species. *Journal of Applied Ecology*, 46(1), pp.46-54.
- Smyth, W.D., Moum, J.N. and Caldwell, D.R. The efficiency of mixing in turbulent patches: Inferences from direct simulations and microstructure observations. *Journal of Physical Oceanography*, 31(8), pp.1969-1992, 2001.

# Turbulent ~~Length-Scale~~Length-scales in a Fast-flowing, Weakly Stratified, Strait: Cook Strait, New Zealand

5

Craig L. Stevens<sup>1,2</sup>

<sup>1</sup> National Institute of Water and Atmospheric Research, Greta Point, Wellington, 6021, New Zealand.

<sup>2</sup> Department of Physics, University of Auckland, New Zealand

10 *Correspondence to:* Craig Stevens ([craig.stevens@niwa.co.nz](mailto:craig.stevens@niwa.co.nz))

← - - Formatted: Affiliation

**Abstract.** There remains much to be learned about the full range of turbulent motions in the ocean. Here we consider turbulence and overturn scales in the relatively shallow, weakly stratified, fast-flowing tidal flows of Cook Strait, New Zealand. With flow speeds reaching  $3 \text{ m s}^{-1}$  in a water column of  $\sim 300 \text{ m}$  depth the location is heuristically known to be highly turbulent.

15 Dissipation rates of turbulent kinetic energy  $\varepsilon$ , along with the Thorpe scale,  $L_T$ , are described. Thorpe scales, often as much as one quarter of the water depth, are compared with dissipation rates and background flow speed. Turbulent energy dissipation rates  $\varepsilon$  are modest but high for oceans, around  $5 \times 10^{-5} \text{ W kg}^{-1}$ . Comparison of the buoyancy-limit Ozmidov scale  $L_O$  suggest the Cook Strait data lie for the majority of the time in the  $L_O > L_T$  regime, but not universally. Also, comparison of direct and  $L_T$ -based estimates of  $\varepsilon$  exhibit reasonable similarity.

← - - Formatted: Font: Not Italic  
Formatted: Font: Not Italic

## 20 1 Introduction

It is well-established that turbulent mixing in the ocean is intermittent and patchy (see Waterhouse et al., 2012<sup>24</sup> for a synthesis). Thus, there is substantial benefit in seeking out extreme conditions to fully capture the global energy budget. Tidal motion, through one pathway or another, drives significant mixing in the ocean. While it is understood that this mixing can 25 influence coastal environmentecological functioning (e.g. Scott et al., 2010; Wesson and Gregg 1994Koch-Larrouy et al., 2015), knowledge gained in shallow coastal situations is also applicable in deeper ocean conditions (e.g. Dale and Inall, 2015). Here we consider these issues in the fast flows of a large tidally-driven passage, Cook Strait, a situation that couples a relatively large vertical extent with large substantial inertial forcing.

In a 1999 paper reviewing the first shear probe measurements of oceanic turbulence Stewart and Grant (1999)<sup>25</sup> described the flows in Seymour Narrows (Discovery Passage, Canada) as sustaining Reynolds Numbers (Re) amongst the "largest in the universe". True or not, it is a useful benchmark and discussion point. There is a tendency to ignore Reynolds number in geophysical flows as they are typically so very large, primarily because of the length-scalelength-scales involved. Cook Strait has comparable flow speeds to Discovery Passage but is around four times the depth, and so suggests a larger bulk Re. From the diapycnal diffusion perspective, despite this highly turbulent large-scalelarge-scale flow, stratification clearly 35 persists through the strait (Stevens, 2014).

← - - Formatted: Indent: First line: 1.27 cm

Of practical concern here is the amount of kinetic energy lost from the system via dissipation (i.e. the rate of dissipation of turbulent kinetic energy,  $\epsilon$ ) as this plays an important role in adequately simulating ocean systems where there is a high dynamic range of variability. This then informs quantification of turbulent diapycnal diffusion which is a balance of turbulent overturning against a stably-stratified background as characterised by the buoyancy frequency squared  $N^2 = (g/p)(dp/dz)$ . Wesson and Gregg (1994) set the scene for the research theme surveying turbulence quantities in the exchange-dominated Straits of Gibraltar where they were able to quantify key turbulence parameters as driven both by internal shear and boundary mixing.

Mater and Venayagamoorthy (2014) lay out a pictorial representation of ~~length-scale~~ in stratified turbulence. The observed Thorpe overturning scale,  $L_T$ , is a relatively measurable quantity associated with ocean structure and can be considered the energy baring scale. This is ~~contained-constrained~~ by the Ozmidov scale ( $L_O = [\epsilon/N^3]^{1/2}$ ) that identifies the limits to growth of eddies and also the Kolmogorov ~~length-scale~~ ( $L_K = [v^3/\epsilon]^{1/4}$ ,  $v$  is kinematic molecular viscosity) where turbulent fluctuations are absorbed by viscous damping forces.

It is common to seek to relate the observable  $L_T$  to mechanically relevant quantities like turbulent kinetic energy,  $\epsilon$ , and its dissipation rate  $\epsilon$  (e.g. Dillon, 1982; Mater et al., 2015). This enables ~~properties estimated from  $\epsilon$  to be estimated~~ from a combination of  $N$  and velocity  $S$  to be inferred from relatively achievable measurements. Recently Mater et al., (2015) and Scotti, (2015) explored the veracity of this long-used approach in a variety of conditions. Typically, however, this has been examined in the deep ocean and so biased away from the more energetic conditions.

The present paper uses microstructure and overturn data to report on the stratified boundary layer response and mixing in the unique situation of Cook Strait as an aid extending our knowledge around oceanic turbulence. It is instructive to compare Cook Strait with other straits of note (Table 1) as it is essentially oceanic, and so relatively weakly stratified, with the  $g'$  in Table 1 being a maximum as observed through an annual cycle. The table includes representative estimates of the Reynolds number and a bulk Richardson number ( $Ri = g'h/\Delta u^2$ ) where  $\Delta u$  is the top-bottom velocity difference ( $Ri \sim 1$  implies weak stratification). The remarkable aspect for Cook Strait is its tidally induced currents and so provides a useful location (Figure 1) because of the very fast tidal flows in reasonably deep water. A number of questions arise: (i) Do we ~~see~~ actually observe high dissipation rates? (ii) How does the Thorpe Scale compare with the Ozmidov Scale? (iii) Following from this, can a fixed ratio be assumed and so allow estimation of  $\epsilon$ ? (iv) How does the turbulence compare with other straits?

## 2 Location and Sampling

Cook Strait, the channel separating New Zealand's North and South Islands, connects the eastern Tasman Sea to the Western Pacific at 42°S (Figure 1). At its narrowest point it is 22 km across, with 210 and 350 m average and maximum depths, respectively. Its fast-flowing tidal currents have been the focus of a number of studies, including the notable observation that the semidiurnal tide is around 140 degrees out of phase when considering the opposite ends of the Strait

(Heath, 1978). This phase difference drives substantial flows, reaching as high as  $3.4 \text{ m s}^{-1}$  during spring tides (Stevens et al. 2012).

Background velocity data come from two instrumented moorings deployed at the “third points” across the narrows (Figure 1) for a period spanning two years, in two deployments, starting in August 2010 and continuing through until 5 September 2012. Each mooring contained an upwards-looking Teledyne-RDI 75 kHz ADCP mounted in a Flotation Technologies syntactic foam float and moored with 600 kg of iron and 10 m of chain. The ADCPs logged at 10 minute intervals, sampling into 8 m depth bins. Each float contained a Seabird microcat (SBE 39) conductivity/temperature/depth sensor placed beneath the ADCPs ~~which~~. ~~The microcats were~~ sampled at 5 minute intervals. This enabled comparison with satellite-derived sea surface temperature for the centre of the strait. With such high ~~tidal~~ flow rates it is not possible to 10 adequately moor instrumentation near the surface as the mooring is “knocked down” meaning that near-surface data are not observed during high flows.

Microstructure profiles were recorded with a VMP500 (Vertical Microstructure Profiler - Rockland Oceanographic, Victoria Canada) instrument. This free-fall, loose-tether package supported two shear probes, two fast thermistors, accelerometers and a Seabird Electronics (SBE) conductivity and temperature sensor-pair. Thirty-four profiles were collected 15 using the 14 m twin-hulled jet-boat Ikatere during a number of expeditions from 2010-2012 ~~but the bulk come from a 12 day period in 2012. The timing of the profiles during the 2012 sampling is shown in Figure 2. It is difficult to capture extended periods of contiguous sampling because a vessel suitably manoeuvrable to conduct the experiments is prone to weather limitations. Sampling over three days in 2012 centered on periods spanning northward, turning and southward tidal flows (Figure 2).~~ It is a particularly challenging environment to profile in, due to the fast flows and strong winds, combined with 20 the relatively long profile durations. A profile and retrieval pair would take around 30 minutes to complete, in which time the vessel would have shifted several km. Keeping the vessel on station was not possible as the line would pay out too far and free-fall would cease. Consequently, sequences of two to three profiles were recorded before repositioning was required.   
 ~~Other sampling strategies have been considered, both as a comparison and as a way to extend the dataset. Ocean glider-mounted microstructure would be affected by the substantial vertical flows. Bed-mounted turbulence sampling will be 25 subject to mooring blow down so that the sampling package will be constantly moving through the vertical. Surface floating gear is affected by the very substantial surface wave field and free-drifting mooring-based sampling is unlikely to get regulatory approval due to the potential for fouling on submarine high voltage DC cables that cross the strait.~~   
 ~~Traditional microstructure profiling thus appears to be a relatively suitable option for now as we seek to capture a greater variety of conditions, especially during the spring tides. The fast flows mean an ability to rapidly reposition is thus an 30 advantage, meaning a smaller vessel in good weather was a better option than a larger vessel able to handle rougher conditions. The end result of all the trade-offs was that we have yet to work out a way to capture a regular sequence of profiles through a~~

tidal cycle in effectively the same location. However we have built up a dataset through all phases of the tide, though only from a limited set of seasonal conditions and not in the very fastest flows.

The profiler captures temperature and conductivity data, however this sensor-pair is un-pumped (to reduce vibration contamination of the shear probe) and so has a slow actual conductivity response and is relatively sensitive to response-time 5 mismatch induced spiking. A fast response conductivity sensor was included in the measurements which gets around the response issue but had its own idiosyncrasies due to fouling and will not be examined here. Correcting un-pumped salinity estimates is becoming more common with ocean glider applications (Timmermans and Winsor, 2013), however the present profiling application is a more rigorous challenge. Being a derivative quantity,  $N^2$  emphasises any spikes or noise. The bulk temperate-salinity relationship for the region is relatively well-ordered and so this enables density for each profile to be 10 calculated using the high quality temperature and theis bulk T-S relationship (for that profile). While this would not be particularly reliable for absolute density estimation, it is sufficient to generate an estimate of the buoyancy frequency squared  $N^2$ . The density profile contains fine-scale overturns and this also results is-in a challenge for  $N^2$  estimation. Mather et al. (2016<sup>5</sup>) review methods for calculating  $N^2$ , and here the patch-average  $N^2$  is used based on a density-sorted profile. The removal of salinity spikes from the original profile data was found to have the greatest impact on the  $N^2$  estimation.

15 \_\_\_\_\_ The microstructure data were recorded using a pair of orthogonally mounted shear sensors. The shear data were recorded at 512 Hz and processed in the usual way to resolve ing the dissipation rate  $\epsilon$  (Wolk et al., 2002; Macoun and Lueck, 2004). This involved first de-spiking to remove spurious transient records, most likely due to encountering biological organisms. The dissipation can then be determined from the integration of shear. However, before this is calculated the useful limit of the data needs to be determined. Unlike many microstructure applications, there is a high signal to noise ratio. What 20 challenges these data is profiler vibration (Wolk et al., 2002). The profiler also samples package motion using a triaxial accelerometer and this provides a cut-off point in the useful shear data, beyond which the spectrum is padded with the Nasmyth spectrum (Macoun and Lueck, 2004). The data were separated into dissipation rate estimates from each of a sensor pair using 5m depth bins. The requirement is that the profiler be passing through the water steadily over the period of any given bin. Vertical speed is resolved from the pressure sensor so that conversion to wavenumber requires reliable velocity estimation 25 (Wolk et al., 2002). Figure 3 shows the profiler drop speed and its variability reflects the degree of vertical turbulent motion which reached as much as  $0.1 \text{ m s}^{-1}$ . The upper portion of the water column includes an acceleration period and sometimes wave effects are apparent. Deeper down it is clear that there is variability in the character of the drop speed variations, although over periods longer than that required for the 5 m vertical bins. The shear spectrum was generated for each depth bin and then compared with a pseudo shear spectrum generated from the accelerometer data. The cross-over point allowed An approach 30 that identification of the noise limit in the shear spectrum above which the signal was and then replaced this with a the Nasmyth model spectrum is applied although with the generally high dissipation rates this was not a particularly dominant significant correction.

Formatted: Superscript

Having resolved  $\epsilon$  and  $N^2$  this then enables a number of derived quantities to be calculated. The Ozmidov scale  $L_{Oz} = (\epsilon/N^3)^{1/2}$  identifies the upper bound at which eddies should “feel” the stratification. One might expect overturns, as identified using the  $L_T$ , to be equal to, or smaller than  $L_{Oz}$ . Dillon (1982) ~~found observed the ratio to be  $L_T/L_{Oz} = 0.8$~~ . This calculation struggles ~~with in regions of low-weak stratification where locally-small  $N^2$  drives results in~~ a very large scale. This 5 makes sense as weak stratification fails to retard turbulence. ~~However, but it can also lead to be~~ non-physical ~~outcomes~~, as the scale will eventually exceed water depth. The vertical (~diapycnal) diffusivity  $K_z$  is commonly calculated as  $K_z = \Gamma \epsilon / N^2$  with  $\Gamma = 0.2$  an assumed constant. While convenient, there is a good deal of evidence to suggest that  $\Gamma$  is not constant ~~for example Bluteau et al. (2013) suggested resulted in an order of magnitude over-estimation of mixing rate and varies between~~. This will be returned to in the Discussion.

10 Given the nature of the salinity structure, as with Wesson and Gregg (1994) and others, we use the more precisely-known temperature to define overturns. The Thorpe scale  $L_T$  is often taken to be some average of displacement scales over a given depth bin. However, this fails to recognise that the enclosed nature of an overturn can set a natural envelope to the estimation (Mather et al., 2015), so that moving through the profile and summing displacements, one can see the start of an overturn and then maintain the sum ~~of~~ displacements until the nett displacement is brought back to zero (within some error). 15 This has the same effect as the centred ~~length scale~~ proposed by Imberger and Boahash (1986) whereby displacements were aggregated at the centre of the overturn. ~~Also by~~ using the microstructure temperature sensor record, the lower limit to this scale is ~~has a not as limited by smaller~~ spatial resolution ~~, as it is with than~~ a traditional CTD thermistor sensor.

## 20 3 Results

The nature of the high flow rates in the strait is illustrated with a day-long sub-section of the two years of velocity data from the eastern side of the Strait (Figure 4~~Figure 3~~). The relatively poor data depth coverage is due to instrument tilt, which while remaining within usable tolerances, does exacerbate side-lobe interference from the surface. While predominantly north-south, the vector sum indicates local speeds reaching  $3 \text{ m s}^{-1}$  at a water depth of around 30 m (speeds above are not 25 known). The flow at this location is not symmetric, with southward flows being 20-50 % smaller.

Vertical velocities reach  $0.1 \text{ m s}^{-1}$  with greater high frequency variability when compared to the horizontal flow signal ~~– this compares with variation observed in profiler drop speed (Figure 3)~~. Backscatter structure has some correlation to the flow speed, with the fast flow periods heralding increased backscatter through most of the measured water column. The bulk velocity shear is described in Stevens (2014) and the asymmetry is particularly clear with levels reaching maximum values of 30  $\pm 0.01 \text{ s}^{-1}$ .

The comparison ~~with of~~ moored ~~and~~ remotely sensed data (Figure 5~~Figure 4~~) suggests that, despite the energetic nature of the strait, it is not fully mixed during the austral summer (Stevens, 2012~~2014~~). The data are insufficient to indicate

if the strait is often stratified in density but it is clearly not homogeneous in temperature for a significant portion of the year. Temperature differences between bed and surface are as large as 3 °C (primarily in the November-April period). Considering the same data in T-S space (Figure 6Figure 5) shows the seabed and surface temperatures span the same range essentially. Three selected microstructure profiles (A, B and C) demonstrate the vertical structure with vertical density differences reaching 5 as high as 0.5 kg m<sup>-3</sup> over the full depth of the water column. The low salinity data ( $S < \sim 34.4$ ) is seen in Stevens (2014) and appears to be results in a 5-month5-month long period at the start of 2012 where the eastern mooring sustained lower  $S$ , but kept a similar T to other moorings at the time. The profiles come from right at the end of this period and so do not exhibit anomalous salinities out of the ordinary.

Before considering the turbulence data en-masse, it is useful to look at the some details of selected some individual profiles. The example profile A (Figure 6Figure 5) is one of the more strongly stratified observed in the strait. The details of this profile (Figure 7Figure 7) illustrate the effect of the conductivity sensor being un-pumped. However, the profile structure at the macroscale is monotonic in temperature and so temperature displacements are dynamically meaningful. Stratification persisted throughout the water column with  $N^2$  being around  $10^{-5} \text{ s}^{-2}$ . Consistent with the relatively constant Neither the  $N^2$ , nor the dissipation rate structure varied greatly through the water column didn't vary greatly. Near-surface values of  $\epsilon$  were 10 low, but increased to hold a near-constant level through most of the water column, then rising near the bed. The large central overturn, as identified with the Thorpe analysis, contained the majority of the vertical variability in  $\epsilon$  in the profile supporting 15 the decision to keep  $L_T$  and  $\epsilon$  calculations separate. The Diffusivity proxy (panel c) will be focused on in the Discussion, however it is notable that in this one instance, the combined  $\epsilon$  and  $N^2$  imply  $K_z$  exceeds  $0.1 \text{ m}^2 \text{s}^{-1}$ , i.e. very large. As will be returned to in the Discussion, Bluteau et al. (2017) find that these large mixing events might themselves be underestimated.

20 The profile B (Figure 8Figure 8) differs from profile A in that it has a large quasi-homogeneous upper portion of the water column. Stratification results in a reduced  $N^2$  being as low as  $10^{-7} \text{ s}^{-2}$  but increasing with depth. The dissipation rate structure increased with depth through the water column (i.e. in tandem with the stratification). The weak stratification was still sufficient that overturn scales were small throughout the water column except for the large upper overturn that exceeds 25 80 m in scale. Interestingly this coincided with an upper layer of low dissipation rate. However, this may be due to a thin low salinity surface layer (c.f. Bowman et al. 1983) with a compensating low temperature, and is a case where density rather than temperature should be used to gauge overturns. In this example, the combined  $\epsilon$  and  $N^2$  imply a  $K_z$  proxy peaking at around 0.1  $\text{m}^2 \text{s}^{-1}$  but mostly an order of magnitude smaller.

25 The final profile example described here, profile C (Figure 9Figure 9), sustains a lower quasi-homogeneous region of the water column. Stratification results in  $N^2$  having a baseline around  $10^{-6} \text{ s}^{-2}$  but significantly increasing at the interface zones. The dissipation rate structure here is bi-modal with a mid-depth minimum. Overturn scales followed the dissipation 30 rate trend with an especially large structure near the bed. Dissipation rates at the bed exceeded  $5 \times 10^{-6} \text{ W kg}^{-1}$ . The variability

Formatted: Font: Not Italic

Formatted: Font: Not Italic

in  $\epsilon$  dominates that of the  $N^2$ , so that the  $K_\epsilon$ -proxy structure mirrors  $\epsilon$  closely, with  $K_\epsilon$  peaking just under  $1 \text{ m}^2 \text{s}^{-1}$  near the bed.

Formatted: Font: Not Italic

This extremely high value is to be expected in a flow known to move large boulders.

#### 4 Discussion

##### 5 Are the dissipation rates actually large?

The distribution of dissipation rate (Figure 10a) shows the level of turbulent kinetic energy (as inferred by  $\epsilon$ ) extends over five orders of magnitude. While the linear average is around  $2 \times 10^{-6} \text{ W kg}^{-1}$ , extrema can exceed  $10^{-4} \text{ W kg}^{-1}$ . In addition, most unusually, there were almost no estimates down at the instrument noise floor around  $10^{-10} \text{ W kg}^{-1}$ . Scaling these estimates over depth, taking the perspective of a numerical modeller looking to resolve friction losses through a Strait, 10 suggests between 0.6 and 30  $\text{W m}^{-2}$  are lost through turbulent dissipation (c.f. say Bab el Mandab of a maximum around 0.2  $\text{W m}^{-2}$ , Jarosz et al. 2005).

It is easy to ignore bulk  $Re$  in ocean physics, assuming correctly that any  $Re$  calculation will be “large”. However, at the turbulence scales buoyancy can potentially affect overturns and re-stratification. The turbulent buoyancy Reynolds 15 number  $Re_b$  ( $= \epsilon / [vN^2]$ ) identifies how velocity fluctuations, and any associated buoyancy flux, evolves and decay. In the present Cook Strait data, the majority of  $Re_b$  estimates exceed 100, with the peak of the distribution being around  $5 \times 10^4$  two orders of magnitude with the peak of the distribution around  $5 \times 10^4$ . (Figure 10b, Figure 14) confirming that the turbulence is “energetic” (Mater et al., 2013). The larger However, maximal  $Re_b$  values exceed  $10^7$ , which is primarily due to the small  $N$ , which approaches the levels of detection. This is larger than the range observed by Wesson and Gregg (1994) who, in the 20 much stronger stratification of Gibraltar, saw more  $Re_b$  values more commonly around  $10^2$ - $10^3$ , but still with high some values  $Re_b$  reaching  $10^5$  or more.

It is a particularly challenging environment to profile in, due to the fast flows and strong winds, combined with the relatively long profile durations. A profile and retrieval pair would take around 30 minutes to complete, in which time the vessel would have shifted as much as several km. Keeping the vessel on station was not possible as the instrument line would 25 pay out too far and so great a distance that line-drag would mean that free-fall would cease. Moving the vessel with the line proved too risky in terms of entanglement. Consequently, sequences of two to three profiles were recorded before repositioning was required the vessel.

Other sampling strategies have been considered, both as a comparison and as a way to extend the dataset. Ocean 30 glider-mounted microstructure would be affected by the substantial vertical flows. Bed-mounted turbulence sampling will be subject to mooring blow-down so that the sampling package will be constantly moving through the vertical. Surface-floating gear is affected by the very substantial surface wave field. In the instance of Cook Strait, and free-drifting mooring-based

sampling is unlikely to get regulatory approval due to the potential for fouling on submarine high voltage DC cables that cross the strait.

Traditional microstructure profiling thus appears to be the most a relatively suitable option for now as we seek to capture a greater variety of conditions, especially during the spring tides. The fast flows mean an ability to rapidly reposition is thus an advantage, meaning a smaller vessel in good weather was a better option than a larger vessel able to handle rougher conditions. The end result of all the trade-offs was that we have yet to work out a way to capture a regular sequence of profiles through a tidal cycle in effectively the same location. However, we have built up a dataset through all phases of the tide, though only from a limited set of seasonal conditions and not in the very fastest flows.

10

#### Does the Thorpe Scale vary systematically with the Ozmidov Scale?

A cross-comparison of  $L_T$  with  $L_{Oz}$  (Figure 11Figure 12) shows a systematic co-variation but one that is far from 1:1. In addition, no  $L_T$  greater than 100 m were observed despite the water column exceeding three-times this and with weak stratification. The calculated  $L_{Oz}$ , on the other hand, is not actually physically constrained and in several instances, it exceeds the water depth. Considering  $\log_{10}$  distributions of  $L_T$  with  $L_{Oz}$ , the observed Thorpe displacement scale  $L_T$  is substantially smaller than the buoyancy-controlled limit  $L_{Oz}$ , by an order of magnitude at smaller length-scales. The two estimates come closest at around  $L_T \sim 10$  m (being around 50% of  $L_{Oz}$ ).

Wesson and Gregg's (1994) observations of turbulence quantities in the Strait of Gibraltar find found that the  $L_{Oz}$  ( $L_B$  in their notation) compares compared essentially 1:1 with  $L_T$ , with most estimates falling within a factor of 4 either side. They also found this degree of scatter held throughout the water column. This differs from that seen here (Figure 12) where the  $L_T$  is substantially smaller than the  $L_{Oz}$  by as much as a decade at smaller scales. The scatter is also larger in the present data as this also is around a decade either side of the mean value. This latter point may be driven by the method used to calculate  $L_T$ . The present noise-rejection conditions mean resulting in that there are fewer very small  $L_{Oz}$  (say  $<0.5$  m) whereas the Gibraltar data drop to as low as  $10^{-2}$  m. In addition, the present use of the microstructure sensors to estimate  $L_T$  allows this to extend to smaller values. Furthermore, The present Cook data exhibit a possible split in behaviour around  $L_{Oz}=10$  m whereas the Gibraltar data only hints at this. Making the same comparison with the Dunkley et al. (2015) Gulf of Aqaba observations ranging over  $L_T=0.1-10$  m, the distribution is almost a mirror reflection around the 1:1 line from that observed in Cook Strait.

In the Gulf of Aqaba results, the  $L_T$  exceeds on average the  $L_{Oz}$  by as much as an order of magnitude – a trend also seen in the Bluteau et al. (2013) data show a similar trend. Finnigan et al. (2002) used the  $L_T$  approach to estimate turbulence in the vicinity of a submarine ridge, and cross-comparison with strain-derived estimates of ~~the~~ suggested it was applicable at least where there was detectable stratification. However, the dissipation rate levels were around  $10^{-9} \text{ W kg}^{-1}$ , three orders of magnitude less than in the present situation.

Formatted: Indent: First line: 1.27 cm

Formatted: Font: Symbol

Formatted: Font: (Default) +Body (Times New Roman)

Formatted: Superscript

Formatted: Superscript

While field studies are typically compromised in some way, complementary analyses through direct numerical simulation (e.g. Smyth et al., 2001) provides supporting evidence that there should be a systematic variation in the empirical overturn scale ( $L_T$ ) and the buoyancy-induced limit to overturns ( $L_{Oz}$ ). This approach suggests that the variation in the ratio of the two scales is an indication of the age of the mixing event, with  $L_{Oz}$  increasing relative to  $L_T$ , and so that scatter in real observations reflects

5 the random age captured by sporadic profiling.

One of the challenges in ocean turbulence is that studies are so intense, focused and idiosyncratic that they tend to be analysed in isolation and rarely synthesized. As a counter-example to this, Mater et al. (2015) collated three open-ocean turbulence experiments from (i) the North Atlantic at around 3000 m (NATRE, Toole et al., 1994), (ii) Brazil Basin mid-Atlantic at around 3000 m (BBTRE, St. Laurent et al., 2001) and (iii) Luzon Straits at around 2500-3000m, (IWISTE, Alford et al., 2011). Here we consider the present data in this context (Figure 12Figure 13). The ratio of  $L_T$  to  $L_{Oz}$  in these deep water experiments was considered against a  $L_T$  non-dimensionalised by the length scale length-scale extracted from viscosity and buoyancy ( $v/N$ )<sup>1/2</sup>, representing the distance momentum can diffuse in a time  $N^{-1}$ . All follow the same trend of the ratio  $L_T/L_{Oz}$  growing with increasing eddy size. All but the NATRE data have significant proportion of data lying with  $L_T < L_{Oz}$ . The present Cook Strait data illustrate this aspect most strongly nearing an order of magnitude smaller at low  $L_T$ .

10 Furthermore, the present data extend into the largest non-dimensional  $L_T$  space. Mater et al. (2015) suggest that while the experiments are deep-water they are still constrained vertically by convective scales.

15

### Does $L_{Oz}/L_T$ allow estimation of $\epsilon$ ?

A comparison of direct shear probe dissipation rate estimates of  $L_{Oz}$   $\epsilon$  and the Thorpe Scale  $L_T$  indicates a broadly comparable trend but that the comparison is not 1:1 (Figure 11Figure 12) with the departure growing for larger scales. There looks to be a bias towards high  $L_T$  values for low  $L_{Oz}$  value at shallow depths. Using the Dillon (1982) approach of assuming taking considering the  $L_{Oz} = [\epsilon/N^3]^{1/2}$  and assuming  $L_{Oz}/L_T$  is fixed such that  $L_{Oz} = aL_T$  then we arrive at a simple expression for  $\epsilon$  (Figure 13Figure 14). This compares the dissipation rates from each  $L_T$  overturn with both the direct and log<sub>10</sub>-based average  $\epsilon$  within that overturn. The direct average (squares) provides a close comparison between observed and estimated  $\epsilon$ . This agreement holds from  $2 \times 10^{-9} \text{ W kg}^{-1}$  through to  $2 \times 10^{-5} \text{ W kg}^{-1}$ , with only one or two departures. The most notable being at  $10^{-9} \text{ W kg}^{-1}$  where it is biased high by a very larger outlier that is so anomalous that it should possibly be discounted. There is an obvious family of outliers in the upper 30 m of water that are anomalously high in terms of the parametrised estimate  $a^2 L_T^2 N^3$  of dissipation rate. Most likely this is a result of some surface-driven stratification effect that either (i) affects turbulence in some systematic way, or (ii) confounds the temperature-based density correction. The log-based comparison is around an order of magnitude smaller. This is included in order to compare this representation with Figure 11Figure 12.

While the  $L_T$  never approaches the full water depth, they are large given the flow speeds. Stevens (2014) measured velocity shear at bulk scales (i.e. resolved from 8 m ADCP bins) reaching as high as  $0.01 \text{ s}^{-1}$ . The velocity variation over an

Formatted: Subscript  
Formatted: Subscript  
Formatted: Subscript  
Formatted: Subscript

Formatted: Superscript

Formatted: Subscript  
Formatted: Font: Not Italic  
Field Code Changed  
Formatted: Font: Not Italic  
Formatted: Font: Not Italic

Formatted: Subscript

Formatted: Superscript

eddy of  $L_e=100$  m in a flow with a velocity shear of  $0.01 \text{ s}^{-1}$  is  $1 \text{ m s}^{-1}$ . This is comparable, but not greater than, background speeds suggesting that it might influence the degree of isotropy by straining eddy structure in the horizontal direction. A similar effect should be expected in slower but much deeper systems such as Bussol Strait (Tanaka et al. 2014; Bryden and Nurser 2003).

Formatted: Subscript

Formatted: Superscript

5

### Implications for, and of, diapycnal diffusion estimatesmixing rate estimates

The  $\Gamma=0.2$  “constant” is a clear point of contention in the literature (e.g. Dunkley et al., 2012; Bluteau et al., 2013; Mashayek et al., 2013). Bluteau et al. (2017) develops an approach that takes microstructure profiles and resolves the diffusivity “directly” fitting a model for dissipation of thermal variance to the convective-inertial subrange (i.e. lower wavenumbers than the dissipation scale). The Bluteau et al. (2017) analysis suggests that improved estimation of the thermal diffusivity indicates that the fixed mixing coefficient might underestimate mixing by a factor of 5 in the mean especially for the more turbulent events. Extending this by applying the Osborne diffusivity method sees an average diffusivity is around  $0.04 \text{ m}^2 \text{ s}^{-1}$  and exceeding  $1 \text{ m}^2 \text{ s}^{-1}$  (Figure 10Figure 10b). One might expect a 300 m water column to then be homogenised in a time ( $L^2/K_z$ )  $300^2/1=25$  hours, but this might be as little as 5 hours if the Bluteau et al. (2017) increased estimate of  $K_z$  were to hold. Tidal excursions due to the semidiurnal tide are insufficient to flush the strait in a single cycle. Indeed, with a net drift of around  $0.02-0.1 \text{ m s}^{-1}$  (Stevens, 2014) it takes many tidal cycles. This suggests that, at these most energetic of mixing conditions, we should not expect to see a stratified water column as it should get mixed over the multiple tidal cycles it takes for water to clear the strait. The bulk top-bottom observations (Figure 5Figure 4) counter this as, for some of the year at least, there is clearly a scalar gradient. Possibly, the observations need to be restructured and collected drifting with the flow to better follow the evolution of mixing.

Formatted: Subscript

Field Code Changed

Lafuente et al. (2013), in their exploration of the impact of vertical diffusion of biologically relevant scalars in the Straits of Gibraltar, found a highly two-dimensional situation whereby the mixing is highly spatially variable, with the presence and location of an internal hydraulic jump being very important. In a similar way to Cook Strait, their simulations show, despite the reasonable tides and strong estuarine circulation, it takes some time for well-mixed water to exit the system. Lafuente et al. (2013) set their background vertical diffusivity to  $10^{-7} \text{ m}^2 \text{ s}^{-1}$  and also prescribed a maximum of  $10^{-2} \text{ m}^2 \text{ s}^{-1}$  in order to “avoid unrealistically high values”. While having the potentially very small  $N^2$  in the denominator for  $K_z$  is problematic, the very large  $\epsilon$  and  $L_T$  make it reasonable to assume, with finite  $N$ , that the larger  $K_z$  estimates are useful in a bulk sense robust. This suggests future work could apply the approach of Bluteau et al. (2017) to profile data to capture the large  $K_z$  events.

Formatted: Subscript

While the focus here is on vertical structure and mixing, the horizontal perspective is also of value. The Strait has been identified as a dividing line in terms of ecological structure (e.g. Forrest et al., 2009). The implication is that there is not a great deal of transverse (across-strait) transport. This supports the focus of the present work on the vertical structure.

Furthermore, over the time it takes to drift through the strait all vessel tracks tended to be on an axis aligned with the strait. Over these scales of time and space the strait itself is bathymetrically reasonable consistent. It remains to conduct a study that will adequately quantify across-strait mixing, the associated drivers and the moderating influence of vertical mixing.

## 5 How does the turbulence compare with other straits?

While the present focus is on turbulent length-scales rather than their oceanographic context. Studies examining flows through stratified straits, both in a net sense and in exchange conditions, classically view the mechanics in terms of non-mixing internal hydraulics (Helffrich, 1995; Hogg et al., 2001). This enables identification of phenomena such as control points and the presence of hydraulic jumps. The extension to consider the role of turbulence and mixing in influencing the system

10 uses bulk estimates of  $K_x$  (Hogg et al., 2001). They were able to demonstrate that by varying the mixing coefficient a strait system could vary between inviscid hydraulic conditions through to a mixing layer. This highlights the need for more direct observations of mixing in such situations.

**Formatted:** Normal, Indent: First line: 1.27 cm, Line spacing: Double

While Stewart and Grant (1999) identify the high Reynolds number in Seymour Narrows (Discovery Passage, British Columbia), it is clear that deeper costal systems like Cook Strait and much deeper oceanic constrictions (e.g. Tanaka et al., 15 2014) create even higher Re conditions. It is difficult to draw general conclusions describing strait behaviour from any one situation as Gregg and Özsoy (2002) noted when quoting Tolstoy to highlight field idiosyncrasies. While the quote was in the context of the Bosphorus, the canonical strait at this scale is probably Gibraltar, the scene of some of the first systematic turbulence quantification (Wesson and Gregg, 1994). These authors state that their 1994 results “rather than being definitive, these results are only the beginning of turbulence measurements in the Strait of Gibraltar”. While this has not really turned 20 out to be the case for Gibraltar, the approach and results spawned a range of studies in comparable systems (Table 1), with the ensemble providing a natural laboratory for exploring a range of ocean mixing phenomena.

### **How does the turbulence compare with other straits?**

It is instructive to compare Cook Strait with other straits of note (Table 1). When doing so it is worth being mindful that Gregg & Özsoy (2002) quoted Tolstoy when relating the unique nature of any given strait. The Tolstoy quote was in the 25 context of the Bosphorus, the canonical strait at this scale is probably Gibraltar, the scene of some of the first systematic turbulence quantification (Wesson and Gregg, 1994). Cook Strait, being essentially oceanic, is relatively weakly stratified, with the  $g'$  in Table 1 being a maximum as observed through an annual cycle.

Wesson and Gregg (1994) state that “rather than being definitive, these results are only the beginning of turbulence 30 measurements in the Strait of Gibraltar”. While this has not really turned out to be the case for Gibraltar, the approach and results spawned a range of studies in comparable systems, with the ensemble providing a natural laboratory for exploring aspects of ocean mixing. In Cook Strait, with its remarkable tides, we intend to improve operational techniques to see if it is

possible to sample during the fastest of the spring tides in order to capture turbulence data in even higher bulk Reynolds number conditions.

## Acknowledgements

5 The author would like to acknowledge colleagues who have aided in the work, in particular Brett Grant, Mark Hadfield, Fiona Elliott, Craig Stewart, Ross Vennell, Murray Smith, Steve Chiswell, Graham Rickard, Rebecca McPherson and Joanne O'Callaghan. Two anonymous Reviewers are thanked for providing constructive comments on an earlier version of this manuscript and Peter Baines is acknowledged for identifying the Tolstoy quote as coming from Anna Kerenina. The support of NIWA Core Funding, and the New Zealand Sustainable Seas National Science Challenge and the Royal Society Te 10 Apārangi Marsden Fund is acknowledged.

## 5 References

Alford, M.H., MacKinnon, J.A., Nash, J.D., Simmons, H., Pickering, A., Klymak, J.M., Pinkel, R., Sun, O., Rainville, L., Musgrave, R. and Beitzel, T.: Energy flux and dissipation in Luzon Strait: Two tales of two ridges. *Journal of Physical Oceanography*, 41(11), pp.2211-2222, 2011.

15 Bluteau, C. E., Jones, N.L. and- Ivey, G.N.: Turbulent mixing efficiency at an energetic ocean site, *J. Geophys. Res. Oceans*, 118, 4662–4672, doi:10.1002/jgrc.20292, 2013.

← - - - Formatted: Indent: Left: 0 cm, Hanging: 1.27 cm

Bluteau, C.E., Lueck, R.G., Ivey, G.N., Jones, N.L., Book, J.W. and Rice, A.E.: Determining mixing rates from concurrent 20 temperature and velocity measurements. *Journal of Atmospheric and Oceanic Technology*, 34, 2283-2293, 2017.

Bowman, M.J., Kibblewhite, A.C., Chiswell, S.M. and Murtagh, R.: Shelf fronts and tidal stirring in Greater Cook Strait, New Zealand. *Oceanologica Acta* 6, 119-129, 1983.

Bryden, H.L. and Nurser, A.G.: Effects of strait mixing on ocean stratification. *Journal of Physical Oceanography*, 33(8), 1870- 1872, 2003.

← - - - Formatted: Font: Not Italic

← - - - Formatted: Font: Not Italic

25 Dale, A. C., and Inall, M.E.: Tidal mixing processes amid small-scale, deep-ocean topography, *Geophys. Res. Lett.*, 42, 484- 491, doi:10.1002/2014GL062755, 2015.

Dillon, T.M.: Vertical overturns: A comparison of Thorpe and Ozmidov length scales. *Journal of Geophysical Research: Oceans*, 87(C12), pp.9601-9613, 1982.

← - - - Formatted: Font: Not Italic

← - - - Formatted: Font: Not Italic

30 Dunckley, J. F., Koseff, J. R., Steinbuck, J.V., Monismith, S.G., and Genin, A.: Comparison of mixing efficiency and vertical diffusivity models from temperature microstructure, *J. Geophys. Res.*, 117, C10008, Doi:10.1029/2012JC007967, 2012.

Finnigan, T. D., Luther, D.S., and Lukas, R.: Observations of enhanced diapycnal mixing near the Hawaiian Ridge. *J. Phys. Oceanogr.*, 32:2988–3002, 2002.

Forrest, B.M., Gardner, J. and Taylor, M.D.: Internal borders for managing invasive marine species. *Journal of Applied Ecology*, 46(1), 46-54, 2009.

5 Frants, M., Damerell, G. M., Gille, S. T., Heywood, K. J., MacKinnon, J., &and Sprintall, J.: An assessment of density-based finescale methods for estimating diapycnal diffusivity in the Southern Ocean. *Journal of Atmospheric and Oceanic Technology*, 30(11), 2647-2661, 2013.

Garrett, C.: Frictional processes in straits. *Deep Sea Research Part II: Topical Studies in Oceanography*, 51(4), pp.393-410, 2004.

Gregg, M.C. and Özsoy, E.: Flow, water mass changes, and hydraulics in the Bosphorus. *Journal of Geophysical Research: Oceans*, 107(C3), 2002.

Heath R.A.: Semidiurnal tides in Cook Strait. *New Zealand Journal of Marine and Freshwater Research*, 12, 87–97, 1978.

Helfrich, K.R.: Time-dependent two-layer hydraulic exchange flows. *Journal of Physical Oceanography*, 25(3), pp.359-373, 1995.

Hogg, A.M., Ivey, G.N. and Winters, K.B.: Hydraulics and mixing in controlled exchange flows. *Journal of Geophysical Research: Oceans*, 106(C1), pp.959-972, 2001.

15 Imberger, J., and Boashash, B.: Application of the Wigner-Ville distribution to temperature gradient microstructure: A new technique to study small-scale variations. *Journal of physical oceanography*, 16(12), 1997-2012, 1986.

Jarosz, E., Teague, W.J., Book, J.W. and Beşiktepe, S.: On flow variability in the Bosphorus Strait. *Journal of Geophysical Research: Oceans*, 116(C8), doi.org/10.1029/2010JC00686, 2011.

Koch-Larrouy, A., Atmadipoera, A., Van Beek, P., Madec, G., Aucan, J., Lyard, F., Grelet, J., and Souhaut, M.: Estimates of tidal mixing in the Indonesian archipelago from multidisciplinary INDOMIX in-situ data. *Deep Sea Research Part I: Oceanographic Research Papers* 106, 136-153, 2015.

25 Lafuente, J. G., Pozas, E. B., Garrido, J. C. S., Sannino, G., &and Sammartino, S.: The interface mixing layer and the tidal dynamics at the eastern part of the Strait of Gibraltar. *Journal of Marine Systems*, 117, 31-42, 2013.

Lu, Y., Lueck, R.G. and Huang, D.: Turbulence characteristics in a tidal channel. *Journal of Physical Oceanography*, 30(5), 855-867, 2000.

30 Lueck, R.G., Wolk, F. and Yamazaki, H., 2002. Oceanic velocity microstructure measurements in the 20th century. *Journal of Oceanography*, 58(1), pp.153-174.

Macoun, P. and Lueck, R.: Modeling the spatial response of the airfoil shear probe using different sized probes. *J. Atmos. Oceanic Technolol.*, 21, 284-297, 2004.

**Formatted:** Font: Not Italic

**Formatted:** Font: 10 pt

Mashayek, A., Caulfield, C.P. and Peltier, W.R.: Time-dependent, non-monotonic mixing in stratified turbulent shear flows: Implications for oceanographic estimates of buoyancy flux. *Journal of Fluid Mechanics*, 736, 570-593, 2013.

5 Mater, B.D., Schaad, S.M. and Venayagamoorthy, S.K.: Relevance of the Thorpe length scale in stably stratified turbulence. *Physics of Fluids*, 25(7), 076604, 2013.

Mater, B.D., Schaad, S.M. and Venayagamoorthy, S.K.: Relevance of the Thorpe length scale in stably stratified turbulence. *Physics of Fluids*, 25(7), p.076604, 2013.

Mater, B. D., and Venayagamoorthy, S. K.: A unifying framework for parameterizing stably stratified shear-flow turbulence. *Physics of Fluids*, 26(3), 036601, 2014.

10 Mater, B.D., Venayagamoorthy, S.K., St. Laurent, L. and Moum, J.N.: Biases in Thorpe-scale estimates of turbulence dissipation. Part I: Assessments from large-scale overturns in oceanographic data. *Journal of Physical Oceanography*, 45(10), 2497-2521, 2015.

Scott, B.E., Sharples, J., Ross, O.N., Wang, J., Pierce, G.J. and Camphuysen, C.J.: Sub-surface hotspots in shallow seas: fine-scale limited locations of top predator foraging habitat indicated by tidal mixing and sub-surface chlorophyll. *Marine Ecology Progress Series*, 408, 207-226, 2010.

15 Scotti, A.: Biases in Thorpe-scale estimates of turbulence dissipation. Part II: energetics arguments and turbulence simulations. *Journal of Physical Oceanography*, 45(10), pp.2522-2543, 2015.

Smyth, W.D., Moum, J.N. and Caldwell, D.R.: The efficiency of mixing in turbulent patches: Inferences from direct simulations and microstructure observations. *Journal of Physical Oceanography*, 31(8), 1969-1992, 2001.

20 Stevens, C.L., Smith, M.J. Grant, B., -Stewart, C.L. and- Divett, T.: Tidal stream energy extraction in a large deep strait: the Karori Rip, Cook Strait, *Continental Shelf Research*, 33, 100-109, 2012.

Stevens, C.: Residual flows in Cook Strait, a large tidally dominated strait. *Journal of Physical Oceanography*, 44(6), pp.1654-1670, 2014.

25 Stewart, R.W. and Grant, H.L.: Early measurements of turbulence in the ocean: Motives and techniques. *Journal of Atmospheric and Oceanic Technology*, 16:1467-1473, 1999.

St. Laurent, L. C., Toole, J. M., & and Schmitt, R. W.: Buoyancy forcing by turbulence above rough topography in the abyssal Brazil Basin\*. *Journal of Physical Oceanography*, 31(12), 3476-3495, 2001.

Tanaka, Y., Yasuda, I., Osafune, S., Tanaka, T., Nishioka, J. and Volkov, Y.N.: Internal tides and turbulent mixing observed in the Bussol Strait. *Progress in Oceanography*, 126, 98-108, 2014.

30 Thorpe, S. A.: Turbulence and mixing in a Scottish loch. *Philosophical Transactions of the Royal Society of London*, A286: 125-181, 1977.

**Formatted:** Font: Not Italic

**Formatted:** Font: Not Italic

**Formatted:** Font: Not Italic

**Formatted:** Font: Not Italic

**Formatted:** Justified, Indent: Left: 0 cm, Hanging: 1.27 cm, Line spacing: Double

**Formatted:** Font: Not Italic

Timmermans, M. L., and Winsor, P.: Scales of horizontal density structure in the Chukchi Sea surface layer. *Continental Shelf Research*, 52, 39-45, 2013.

**Formatted:** Font: Not Italic

Toole, J.M., Schmitt, R.W. and Polzin, K.L.: Estimates of diapycnal mixing in the abyssal ocean. *Science*, 264(5162), 1120-1123, 1994

**Formatted:** Font: Not Italic

5 Vennell, R.: Acoustic Doppler Current Profiler measurements of tidal phase and amplitude in Cook Strait, New Zealand. *Continental Shelf Research*, 14, 353-364, 1994.

Vennell, R.: Observations of the phase of tidal currents along a strait. *Journal of physical oceanography*, 28(8), 1570-1577, 1998.

**Formatted:** Font: Not Italic

**Formatted:** Font: Not Italic

Waterhouse, A.F., MacKinnon, J.A., Nash, J.D., Alford, M.H., Kunze, E., Simmons, H.L., Polzin, K.L., St. Laurent, L.C., 10 Sun, O.M., Pinkel, R. and Talley, L.D.: Global patterns of diapycnal mixing from measurements of the turbulent dissipation rate. *Journal of Physical Oceanography*, 44, 1854-1872, 2014.

Wesson, J. C., and M.C. Gregg: Mixing at Camarinal Sill in the Strait of Gibraltar, *J. Geophys. Res.*, 99, 9847-9878, 1994.

Wolk, F. H. Yamazaki, L. Seuront, R. G. Lueck: A new free-fall profiler for measuring biophysical microstructure. *J. Atmos. Oceanic Technol.*, 19, 780-793, 2002.

15

Table 1 Comparison of approximate representative strait scales (modified-extended from Helffrich, 1995 and Hogg et al. 2001)

Strait	$g'/m s^2$	Depth m	$U m s^{-1}$	Length km	Re	Ri	Source
Cook	0.006	350	3.0	40	$10^9$	0.9	Present study; Stevens (2014)
Bosphorus	0.12	35	0.8	30	$3 \times 10^7$	2.1	Gregg and Özsov (2002)
Cordova	0.003	30	0.9	3	$3 \times 10^7$		Lu et al. (2000)
Seymour Narrows	0.02	60280	4.2 (M <sub>2</sub> )6	320	$3 \times 10^8 4 \times 10^8$	3.6	Stewart and Grant 1999; Lueck et al. (2002)
Gibraltar	0.02	280	1.2	20	$4 \times 10^8$	3.6	Wesson and Gregg (1994)
Bussol	0.01	1750	1.0	~50	$10^9$		Tanaka et al (2014)

5

**Formatted:** Font: 11 pt  
**Formatted:** Font: 11 pt  
**Formatted:** Line spacing: single  
**Formatted:** Left, Indent: Left: 0.31 cm, Line spacing: single  
**Formatted Table**  
**Formatted:** Font: 11 pt  
**Formatted:** Line spacing: single  
**Formatted:** Left, Indent: Left: 0.31 cm, Line spacing: single  
**Formatted:** Font: 11 pt  
**Formatted:** Line spacing: single  
**Formatted:** Left, Indent: Left: 0.31 cm, Line spacing: single  
**Formatted:** Font: 11 pt  
**Formatted:** Line spacing: single  
**Formatted:** Left, Indent: Left: 0.31 cm, Line spacing: single  
**Formatted:** Line spacing: single  
**Formatted:** Left, Indent: Left: 0.31 cm, Line spacing: single  
**Formatted:** Line spacing: single  
**Formatted:** Left, Indent: Left: 0.31 cm, Line spacing: single  
**Formatted:** Line spacing: single  
**Formatted:** Left, Indent: Left: 0.31 cm, Line spacing: single  
**Formatted:** Line spacing: single  
**Formatted:** Superscript  
**Formatted:** Left, Indent: Left: 0.31 cm, Line spacing: single

## Figures

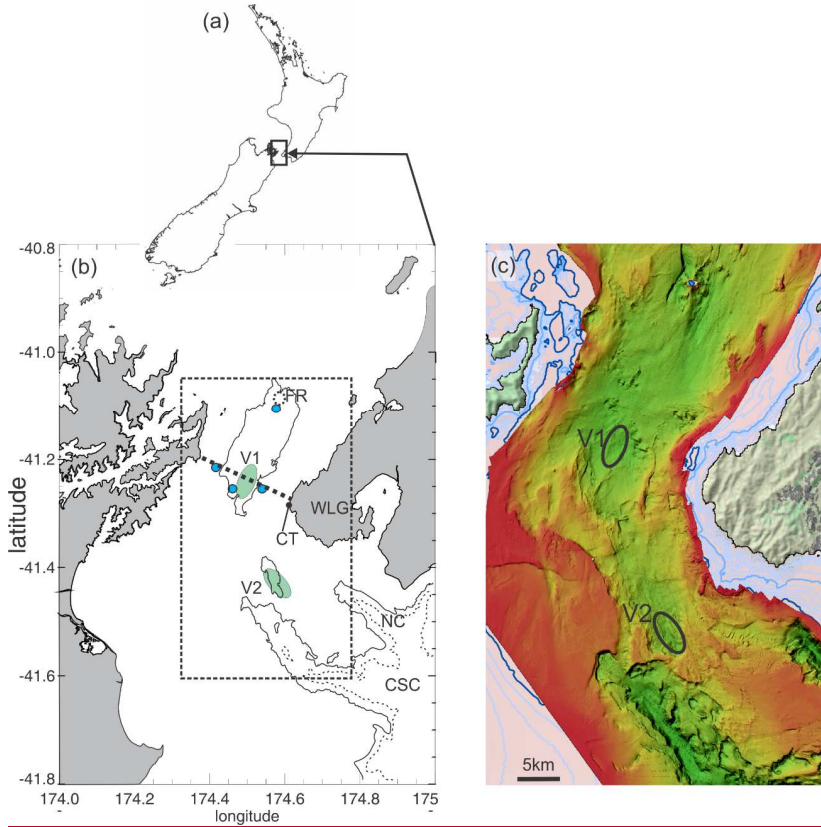


Figure 1 Location showing (a) New Zealand, and within this, (b) Cook Strait Narrows is bounded by Cape Terawhiti (CT) to the east and the headlands of the (shaded) Marlborough Sounds to the west and with the Cook Strait and Nicholson Canyons to the south (CSC and NC).

5 The 200 m (solid) and 400 m (dashed) depth contours are marked, as well as the shoal at Fishermans Rock (FR). ADCP moorings are marked with blue circles. The microstructure data come from profile regions V1 and V2.

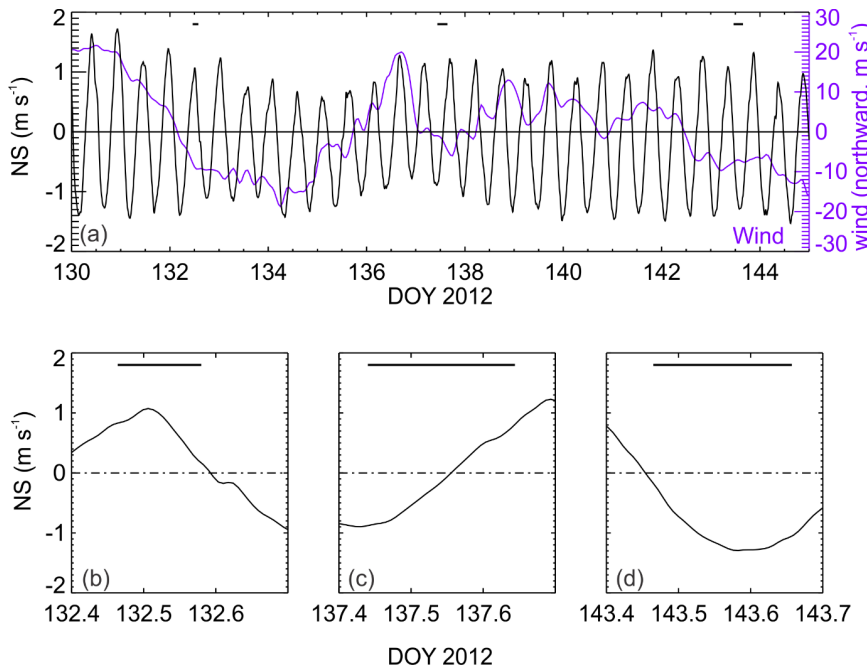
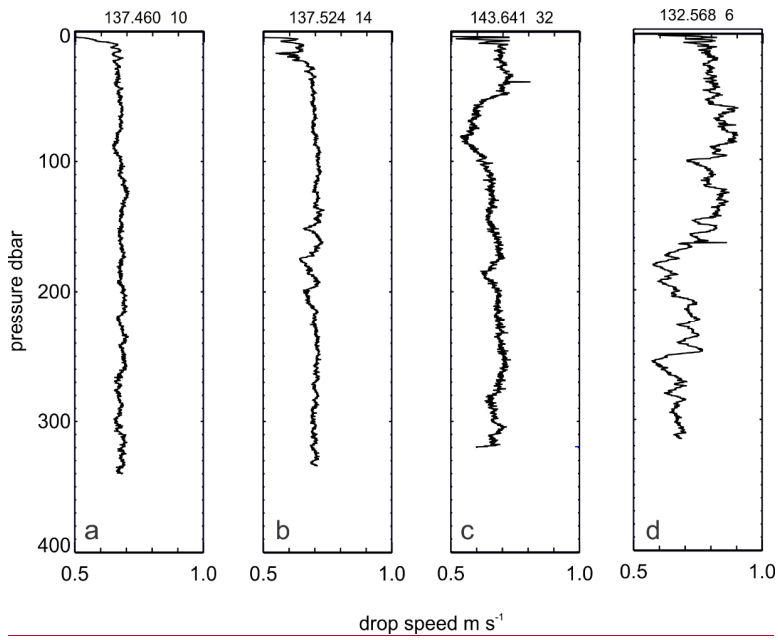


Figure 2 Sampling conditions showing average N-S water column velocity between 60 and 100 m depth and wind speed - both filtered with an hourly low-pass filter. The bars show microstructure sample periods. These bars are expanded in the daily sampling relative to tidal conditions is shown in (b), (c) and (d).

5 [Figure 6 – sampling conditions average N-S velocity between 60 and 100 m depth and wind speed both filtered with an hourly low-pass filter. The bars show sample periods.](#)



[Figure 3](#) profiler drop speed from a number of example profiles (time and profile number on top).

[Figure 2](#) profiler drop speed from a number of example profiles.

← - - **Formatted:** Caption, Line spacing: single, Don't keep with next

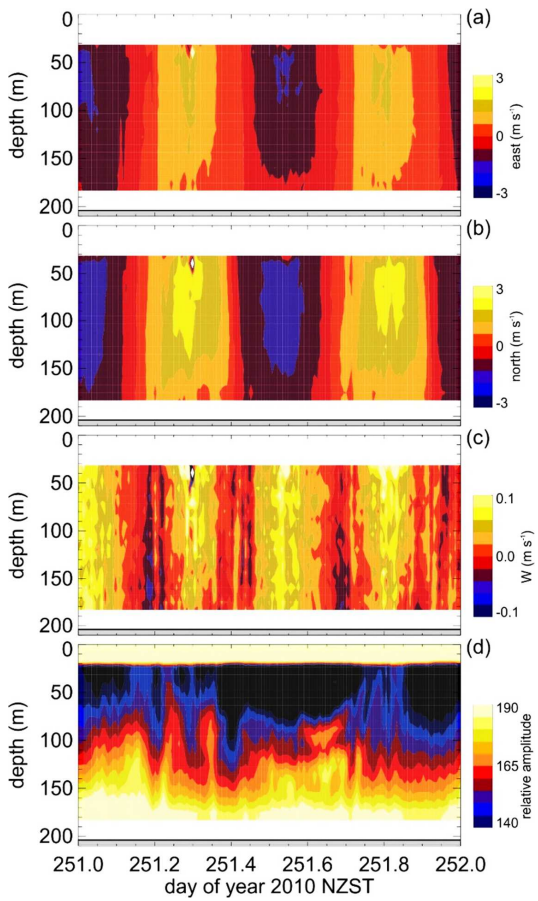


Figure 4 velocity data from eastern side of strait showing (a) east-west, (b) north-south, (c) vertical velocities and (d) backscatter amplitude. Formatted: Keep with next

Figure 3 velocity data from eastern side of strait showing (a) east-west, (b) north-south, (c) vertical velocities and (d) backscatter amplitude.

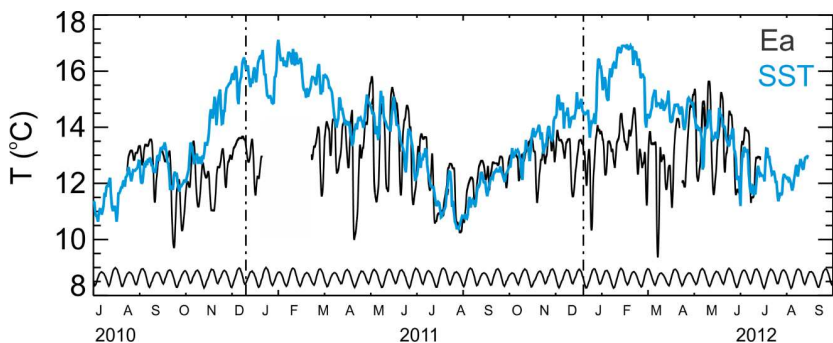


Figure 5 Temperatures from near-bed (Ea, Figure 1) and satellite-derived sea surface temperature (SST). The arbitrarily-scaled spring-neap envelope is along the base of the panel.

Formatted: Caption, Line spacing: single  
Field Code Changed

5 Figure 4 Temperatures from near-bed (Ea, Figure 1) and satellite-derived sea surface temperature (SST). The arbitrarily-scaled spring-neap envelope is along the base of the panel.

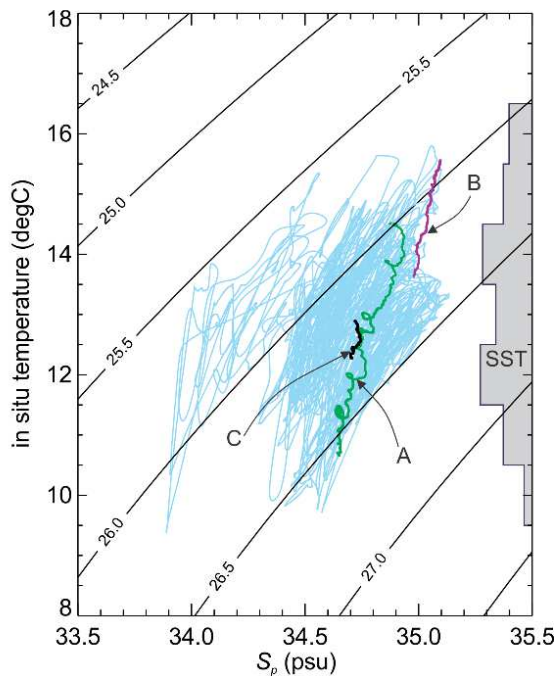


Figure 65 Temperature and salinity ( $S_p$ ) from the seabed sensors on the moorings with profile data overlain (see text for details) and  $\sigma_1$  contours. The arbitrary-scaled [distribution histogram](#) on the right-hand margin shows the distribution of satellite-derived sea surface

5 temperature (SST).



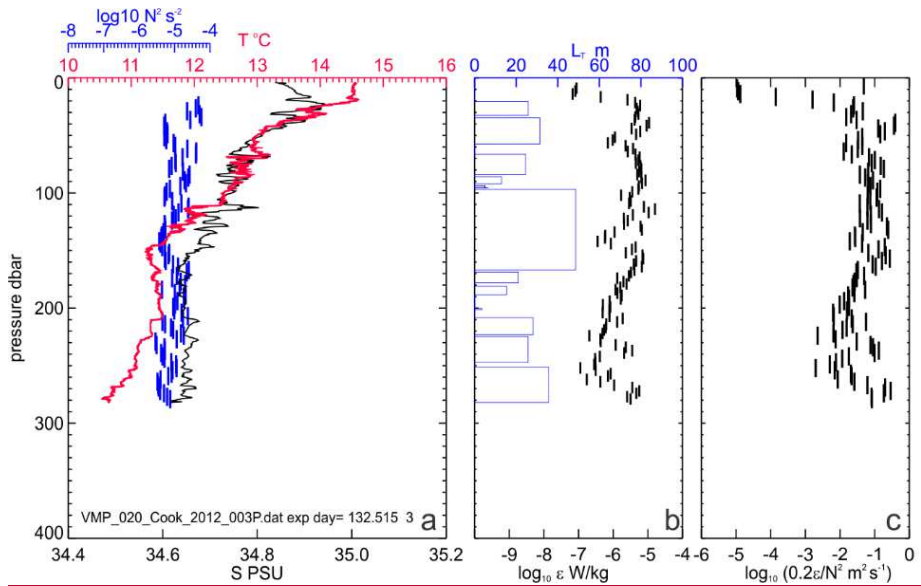


Figure 27 Profile A from day 132, 2012 showing (a) temperature, salinity and buoyancy frequency squared ( $N^2$ )-squared, (b)

$L_T$  and  $\epsilon$  and (c) proxy for vertical diffusivity  $0.2\epsilon/N^2$ . Note the profile extends over the full depth of the water column.

Formatted: Font: Symbol

Formatted: Superscript

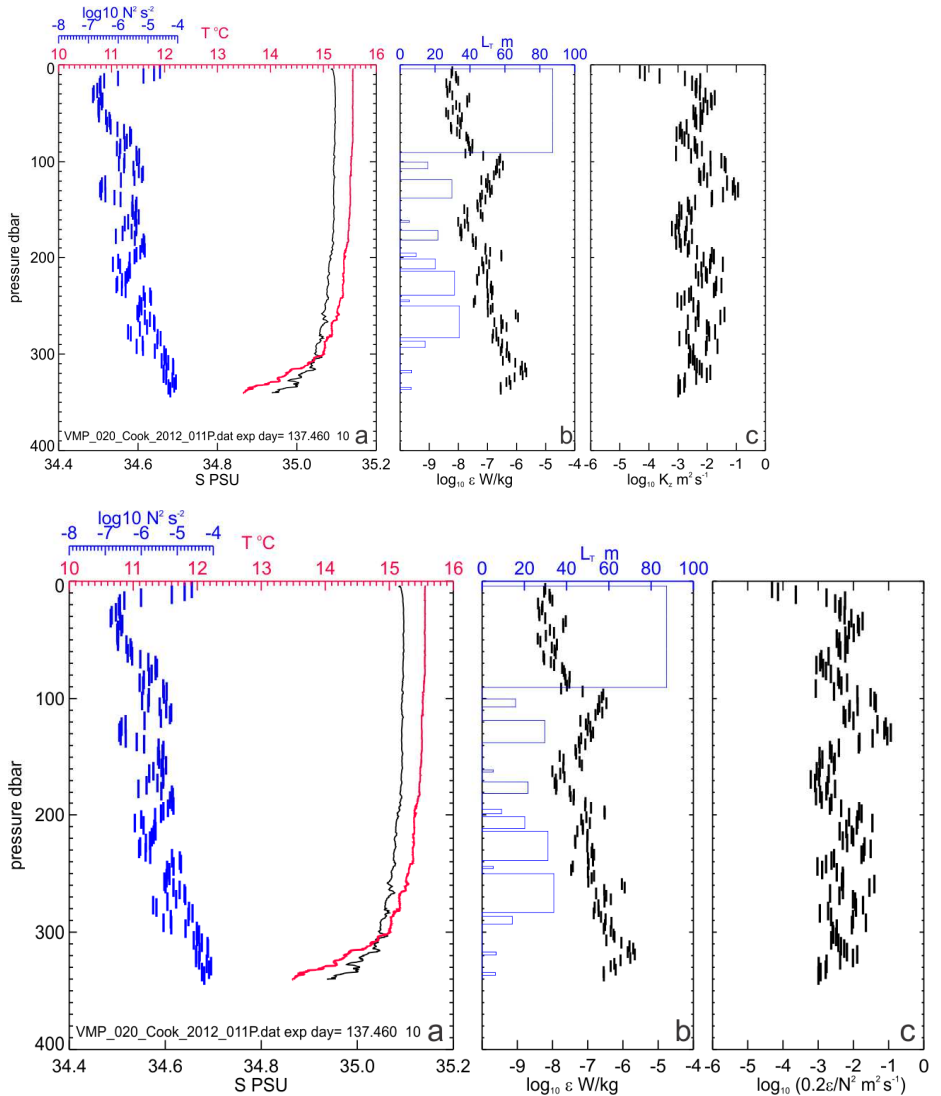
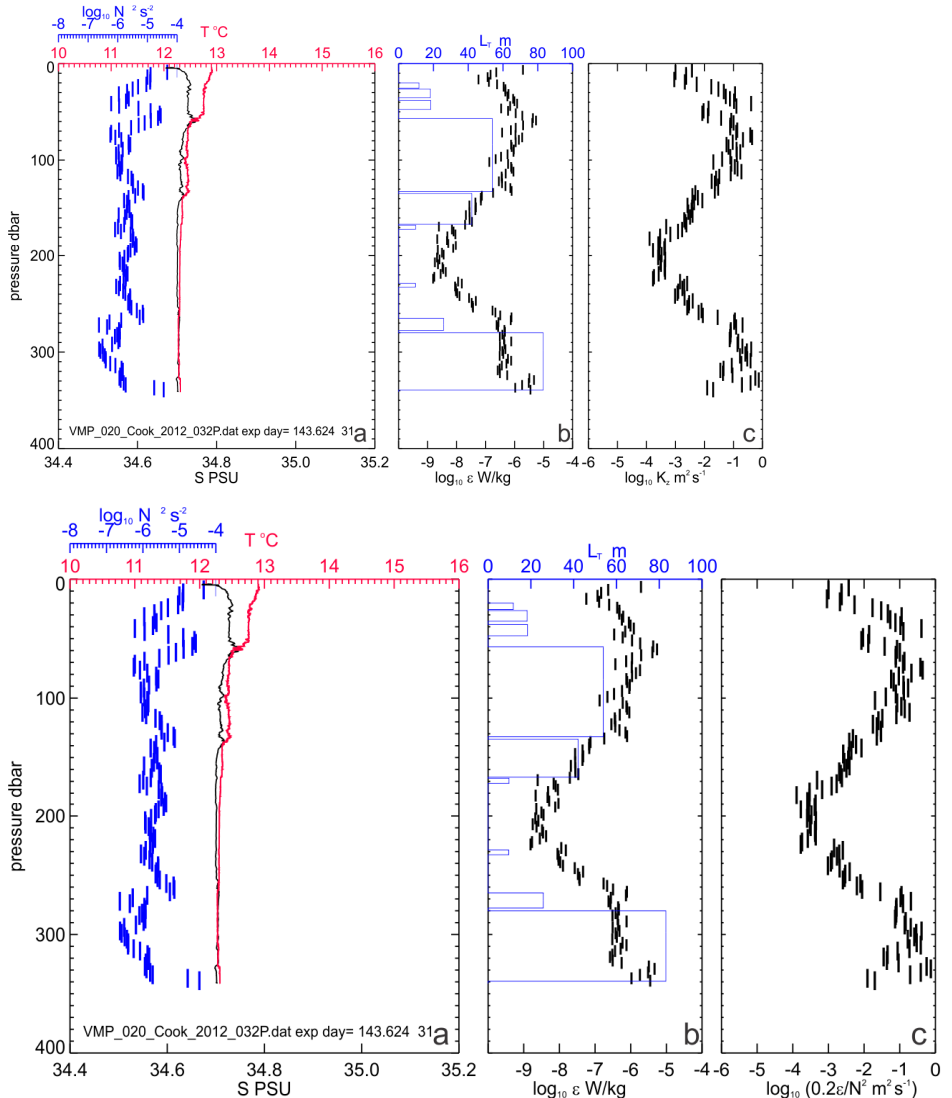


Figure 88 Profile B from day 137, 2012 showing (a) temperature, salinity and buoyancy frequency squared ( $N^2$ ), (b)  $L_T$  and  $\epsilon$  and (c) proxy for vertical diffusivity  $0.2\epsilon/N^2$ . Note the profile extends over the full depth of the water column showing (a) temperature, salinity and buoyancy frequency ( $N^2$ ) squared, (b)  $L_T$  and  $\epsilon$  and (c) vertical diffusivity  $K_v$ . Note the profile extends over the full depth of the water column.



5 Figure 99 Profile C from day 143, 2012 showing (a) temperature, salinity and buoyancy frequency squared ( $N^2$ ), (b)  $L_T$  and  $\epsilon$  and (c) proxy for vertical diffusivity  $0.2\epsilon/N^2$ . Note the profile extends over the full depth of the water column showing (a) temperature, salinity and buoyancy frequency ( $N^2$ ) squared, (b)  $L_T$  and  $\epsilon$  and (c) vertical diffusivity  $K_v$ . Note the profile extends over the full depth of the water column.

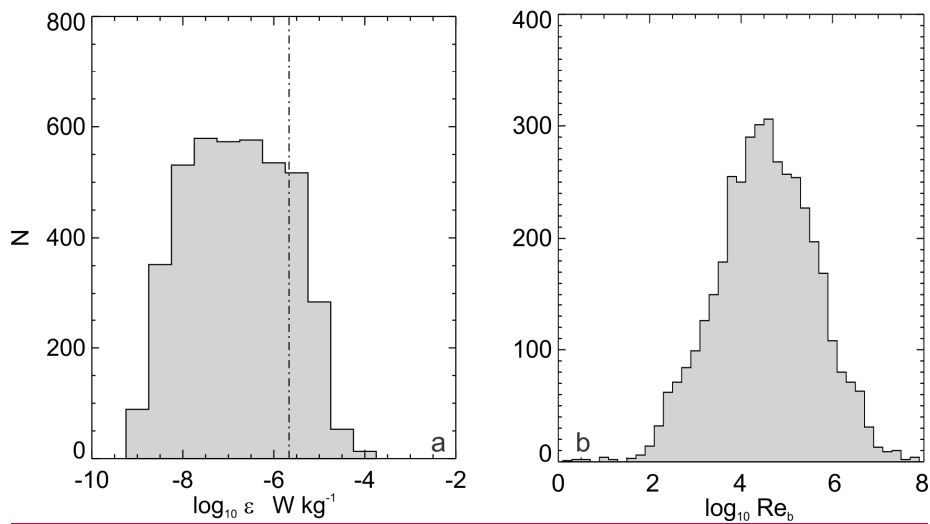
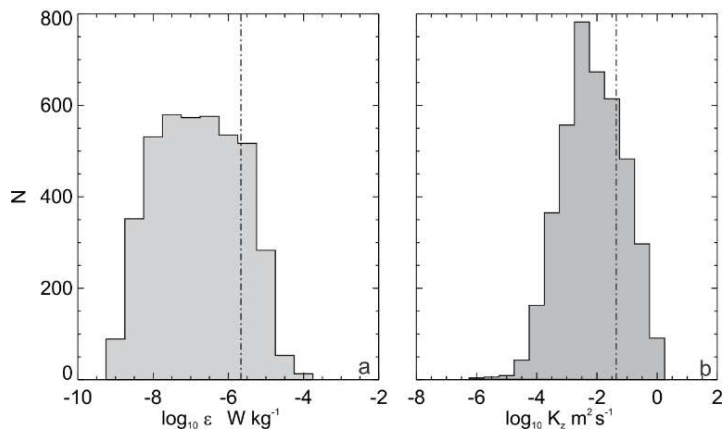
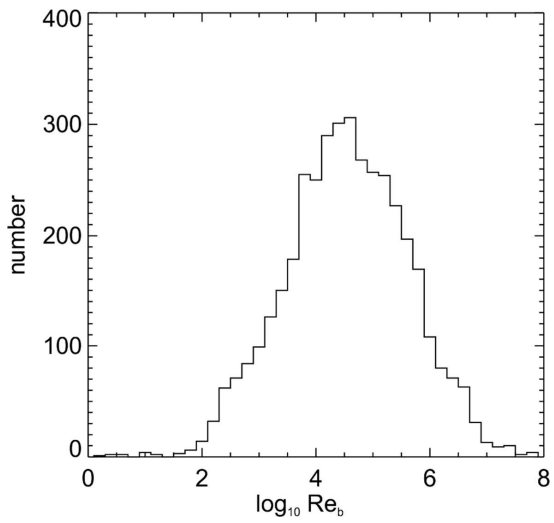


Figure 1040 Distributions of (a) dissipation rate  $\varepsilon$  and (b) [buoyancy Reynolds number,  \$Re\_b\$](#) , [inferred vertical diffusivity  \$K\_z\$](#) .



5 Figure 11 Distribution of buoyancy Reynolds number,  $Re_b$

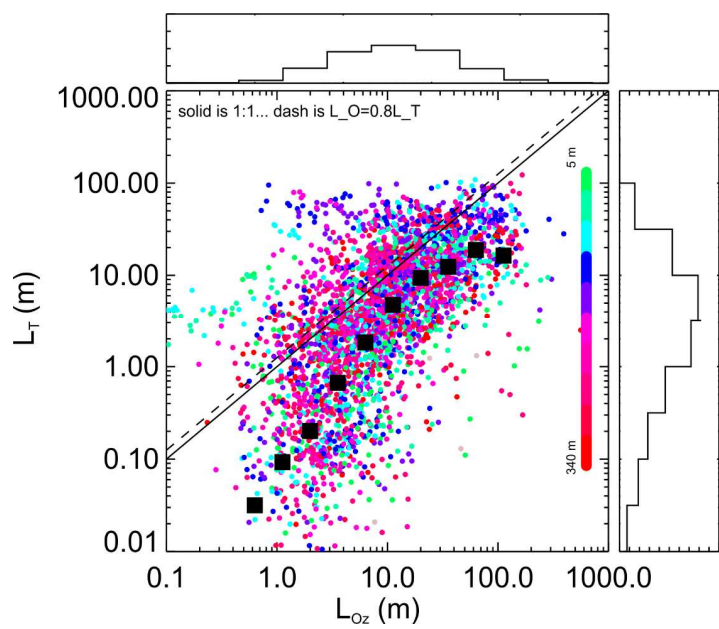


Figure 1142 Scatter plot of  $L_T$  vs  $L_{Oz}$  colour-coded by depth. Lines for unity and for  $L_{Oz}=0.8L_T$  are shown and associated histograms of length-scales are shown also. Averages were calculated in log10 space and 0.5 m was considered a lower-bound for  $L_{Oz}$ .

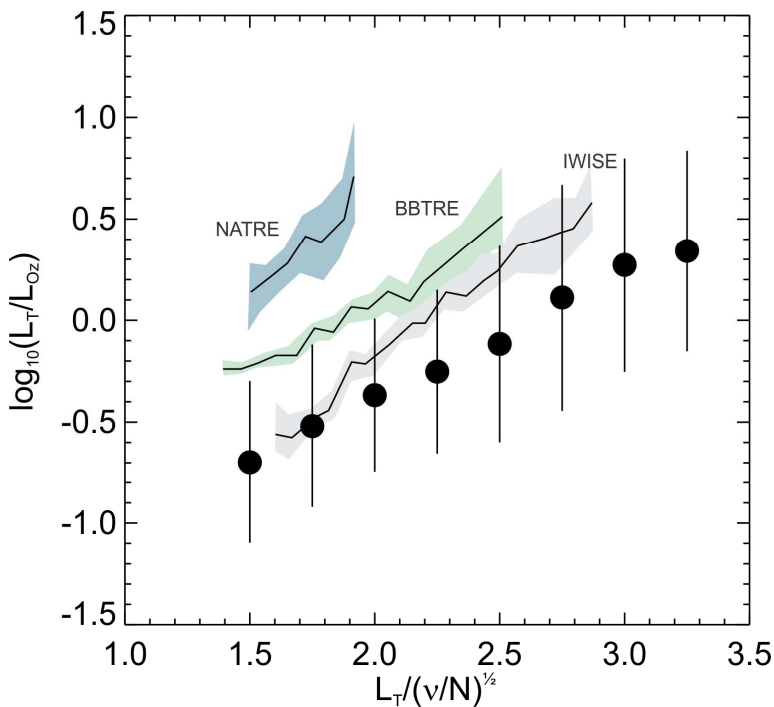


Figure 1243 The comparison of the  $L_r/Lo_z$  ratio as a function on non-dimensionilised  $L_r$ . The present data set (circles with  $\pm 1$  standard deviation as error bars) is superposed on top of synthesized results following Mater et al (2015).

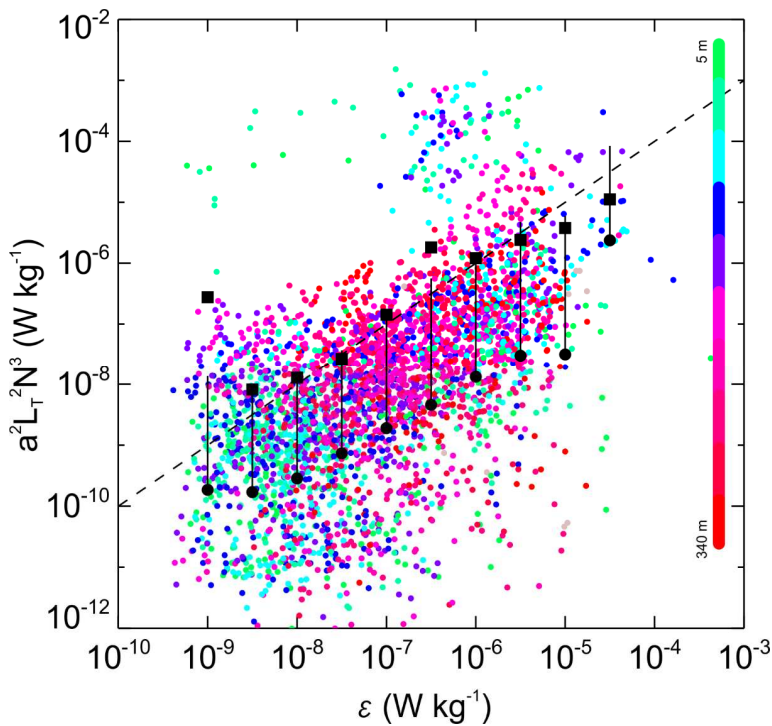


Figure 134 Comparison of dissipation resolved from the  $Lo_z$  with the direct measure of  $\epsilon$ . Averages were calculated in log10 space for  $\epsilon$  and all length-scale-based estimates in that bin were collated. Here the average and average+ 1 standard deviation are shown with a circle-line pair and the average in log10 space is shown as a square. The averages excluded outliers in the surface water as described in the text.